Photoinduced electron transfer in a clicked fullerene–porphyrin conjugate†‡

Julien Iehl,[a] Maida Vartanian,[a] Michel Holler,[a] Jean-François Nierengarten,*[a] Béatrice Delavaux-Nicot,*[b] Jean-Marc Strub,[c] Alain Van Dorsselaer,*[c] Yilei Wu,[d] John Mohanraj,[d] K. Yoosaf[d] and Nicola Armaroli*[d]

Received 16th July 2010, Accepted 8th October 2010
DOI: 10.1039/c0jm02310h

A stable C_{60} derivative bearing an azide functional group has been prepared and used as a building block for the preparation of a fullerene–porphyrin conjugate (**F–P–F**) by reaction with a Zn(II)–porphyrin bearing two terminal alkyne groups under the copper mediated Huisgen 1,3-dipolar cycloaddition conditions. The electrochemical and photophysical properties of the resulting multicomponent system have been investigated in detail. In benzonitrile, **F–P–F** undergoes photoinduced electron transfer and the resulting charge separated state is relatively long lived ($\tau = 0.48$ μs). In contrast, intramolecular energy transfer has been evidenced in toluene, with the generation of the fullerene triplet level upon selective excitation of the porphyrin moiety. In this solvent, a CT emission band is observed in the near-infrared region ($\lambda_{max} = 940$ nm) as a consequence of a conformational equilibrium causing, to a minor extent, the formation of intramolecular porphyrin–fullerene tight pairs. This finding is supported by measurements of singlet oxygen sensitization and quenching of the long-lived fullerene centered triplet state in the oxygen free solution.

Introduction

Owing to their specific electronic properties, fullerene derivatives are attractive photo- and electro-active components in artificial photosynthetic systems.[1–3] Among the numerous fullerene-based photoactive molecular devices reported so far,[1] systems combining fullerene accepting moieties with porphyrin donors have generated a great deal of attention.[2] Spectacular covalent and non-covalent fullerene–porphyrin conjugates have been already prepared and systematic studies of their electronic properties revealed interesting photoinduced processes.[2] Importantly, accelerated charge separation and decelerated charge recombination have been evidenced in a fullerene-based acceptor–donor system when compared to the equivalent benzoquinone-based system.[4] This has been interpreted by the smaller reorganization energy (λ) of C_{60} when compared with those of small acceptors.[4] The efficient photogeneration of long lived charge-separated states by photoinduced electron transfer in fullerene–porphyrin systems is particularly interesting for solar energy conversion. Indeed, photovoltaic devices prepared from such hybrid compounds have shown promising energy conversion efficiencies.[3] On the other hand, strong attractive fullerene–porphyrin interactions have been evidenced for several covalent and non-covalent C_{60}–porphyrin derivatives,[5] as well as in the solid state structures of porphyrin/fullerene co-crystals.[6] The establishment of such intramolecular π-stacking interactions between the two chromophores has been demonstrated spectroscopically both in the ground and in the excited state. In particular, charge transfer (CT) excited state levels in the near-infrared (NIR) region have been evidenced, which are typically the funnel of the excitation energy initially addressed to upper electronic states localized on each chromophore.[7]

As part of this research, we have developed versatile fullerene–benzaldehyde building blocks for the construction of functionalized porphyrins bearing multiple fullerene residues.[8] More recently, we have also reported the synthesis of fullerene–porphyrin conjugates from clickable building blocks.[9,10] In particular, we have shown that the copper mediated Huisgen 1,3-dipolar cycloaddition of organic azides and terminal alkynes[11] leading to 1,2,3-triazoles is a perfectly suited tool for fullerene chemistry.[12,13] In this paper, we now report a full account on the synthesis of a C_{60}–porphyrin conjugate from a fullerene–azide building block and a porphyrin derivative bearing alkyne units. The electrochemical and photophysical properties of the hybrid compound have been investigated in detail.

Interestingly, a NIR charge transfer emission has been observed in toluene, suggesting that the C_{60}–porphyrin derivative adopts, though to a minor extent, a folded conformation that allows π–π interactions between the fullerene subunits and the central porphyrin moiety. The majority of the molecules adopt a more extended conformation in which photoinduced energy transfer and electron transfer are observed in toluene and benzonitrile, respectively.

[a]*Laboratoire de Chimie des Matériaux Moléculaires, Ecole Européenne de Chimie, Polymères et Matériaux, Université de Strasbourg et CNRS (UMR 7509), 25 rue Becquerel, 67087 Strasbourg Cedex 2, France. E-mail: nierengarten@chimie.u-strasbg.fr*
[b]*Laboratoire de Chimie de Coordination du CNRS, Université de Toulouse (UPS, INP), 205 route de Narbonne, 31077 Toulouse Cedex 4, France. E-mail: Beatrice.Delavaux-Nicot@lcc-toulouse.fr*
[c]*Laboratoire de Spectrométrie de Masse Bio-organique, Institut Pluridisciplinaire Hubert Curien (IPHC), Ecole Européenne de Chimie, Polymères et Matériaux (ECPM), Université de Strasbourg et CNRS (UMR 7178), 25 rue Becquerel, 67087 Strasbourg Cedex 2, France. E-mail: vandors@chimie.u-strasbg.fr*
[d]*Istituto per la Sintesi Organica e la Fotoreattività, Consiglio Nazionale delle Ricerche, via Gobetti 101, 40129 Bologna, Italy. E-mail: armaroli@isof.cnr.it*

† Electronic supplementary information (ESI) available: 2D NOESY spectrum of **F-P-F**; OSWVs of **F** and **12**; singlet oxygen luminescence spectra and differential transient absorption spectra of **P**, **F** and **F-P-F**. See DOI: 10.1039/c0jm02310h

‡ Dedicated to Prof. F. Wudl on the occasion of his 70th birthday.

Results and discussion

Synthesis

The preparation of the fullerene–azide building block is depicted in Scheme 1. This compound was obtained by taking advantage of the regioselective reaction developed in the group of Diederich,[14] which led to macrocyclic bis-adducts of C_{60} by a cyclization reaction at the fullerene sphere with a bis-malonate derivative in a double Bingel[15] cyclopropanation. To this end, we have first prepared bis-malonate **6** bearing an azide group. Reaction of phenol **1**[16] with tosylate **2**[17] and K_2CO_3 in DMF at 80 °C afforded **3** which after treatment with tetrabutylammonium fluoride (TBAF) gave diol **4**. *N*,*N*′-Dicyclohexylcarbodiimide (DCC)-mediated esterification of **4** with the malonic mono-ester **5**[18] yielded bis-malonate **6**. It is worth noting that the 3,5-didodecyloxybenzyl groups introduced at this stage should prevent any solubility problems for the targeted fullerene derivatives. Indeed, this group has already proven to be an excellent solubilizing group for C_{60} derivatives.[19]

Treatment of C_{60} with **6**, iodine and 1,8-diazabicyclo[5.4.0]undec-7-ene (DBU) in toluene at room temperature afforded the *cis*-2 bis-adduct **7** in 56% yield. As shown in Fig. 1, the ^{1}H NMR spectrum of **7** reveals the characteristic features of C_s symmetrical 1,3-phenylenebis(methylene)-tethered fullerene *cis*-2 bis-adducts.[20] Effectively, two AB quartets are observed for the two sets of diastereotopic benzylic CH_2 groups (H–A/B and H–C/D) and an AX_2 system is revealed for the aromatic protons of the 1,3,5-trisubstituted bridging phenyl ring (H-3/4). The ^{13}C NMR spectrum of **7** is also in full accordance with the proposed molecular structure. In particular, four of the resonances seen between δ = 134 and 148 ppm for the different fullerene sp^2 C atoms show half intensity (δ = 134.6, 138.0, 147.5 and 147.6). Actually, the latter observation is an unambiguous proof for the C_s symmetry[20] of compound **7**. Effectively, for such a C_{60} derivative, there are 26 pairs of equivalent sp^2 fullerene C atoms and four unique ones. Additionally, the orange-red color and the UV/Vis spectrum of **7** are fully consistent with those of previously reported analogous *cis*-2 bis-adducts.[21] Indeed, the absorption spectra of C_{60} bis-adducts are characteristic for each of the regioisomers.[14,22] It is also well-established that the 1,3-phenylenebis(methylene)-tethered bis-malonates produce regioselectively the C_s symmetrical *cis*-2 addition pattern at C_{60}.[14,20,21] It is also worth noting that fullerene azide derivative **7** is a quite stable compound under normal laboratory conditions. A sample was stored in the fridge for several months without any detectable decomposition. The latter observation is quite unusual for fullerene–azide derivatives for which intermolecular cycloaddition reactions between the C_{60} and the azide groups led generally to fast decomposition.[12] The remarkable stability of compound **7** may be the result of the encapsulation of the fullerene sphere in its cyclic addend surrounded by two 3,5-didodecylbenzyl ester moieties thus preventing the reaction of the azide group with the C_{60} core.

The functionalization of building block **7** under the copper-catalyzed 1,3-dipolar cycloaddition was first attempted with phenylacetylene. The reaction conditions were the same as the one we optimized for the click reactions of azides with fullerene–alkyne derivatives.[12] Treatment of compound **7** with

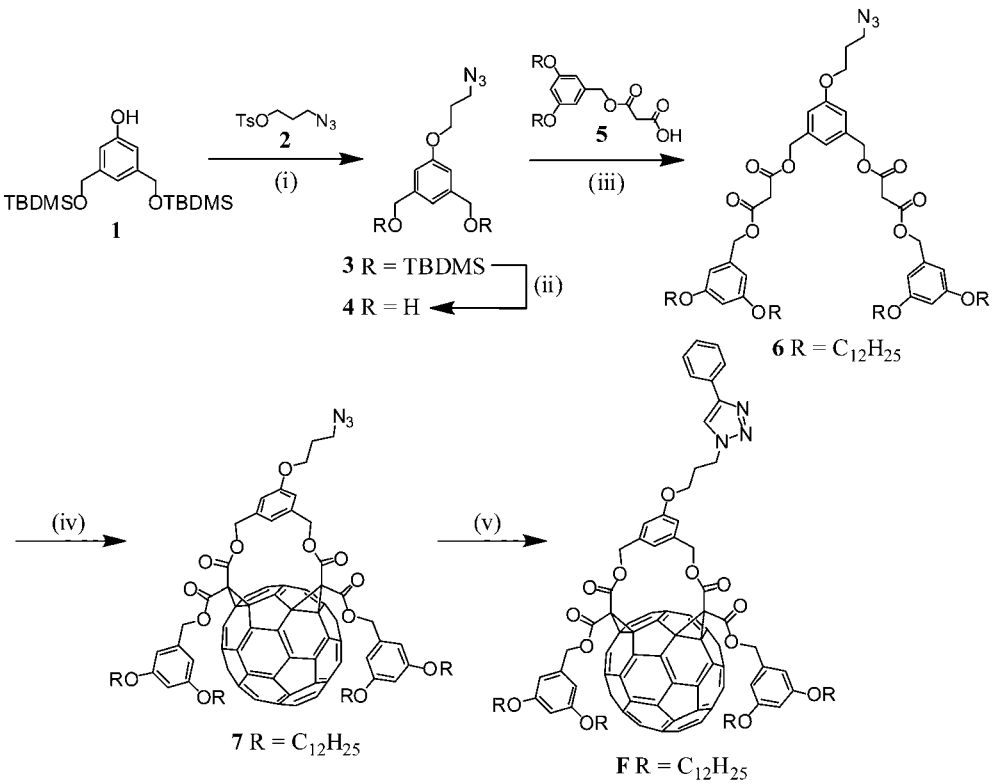

Scheme 1 *Reagents and conditions*: (i) K_2CO_3, LiBr, DMF, 80 °C, 96 h (33%); (ii) TBAF, THF, 0 °C, 3 h (73%); (iii) DCC, DMAP, HOBt, CH_2Cl_2, 0 °C to rt, 72 h (65%); (iv) C_{60}, DBU, I_2, PhMe, rt, 12 h (56%); (v) phenylacetylene, $CuSO_4 \cdot 5H_2O$, sodium ascorbate, CH_2Cl_2/H_2O, rt, 16 h (73%).

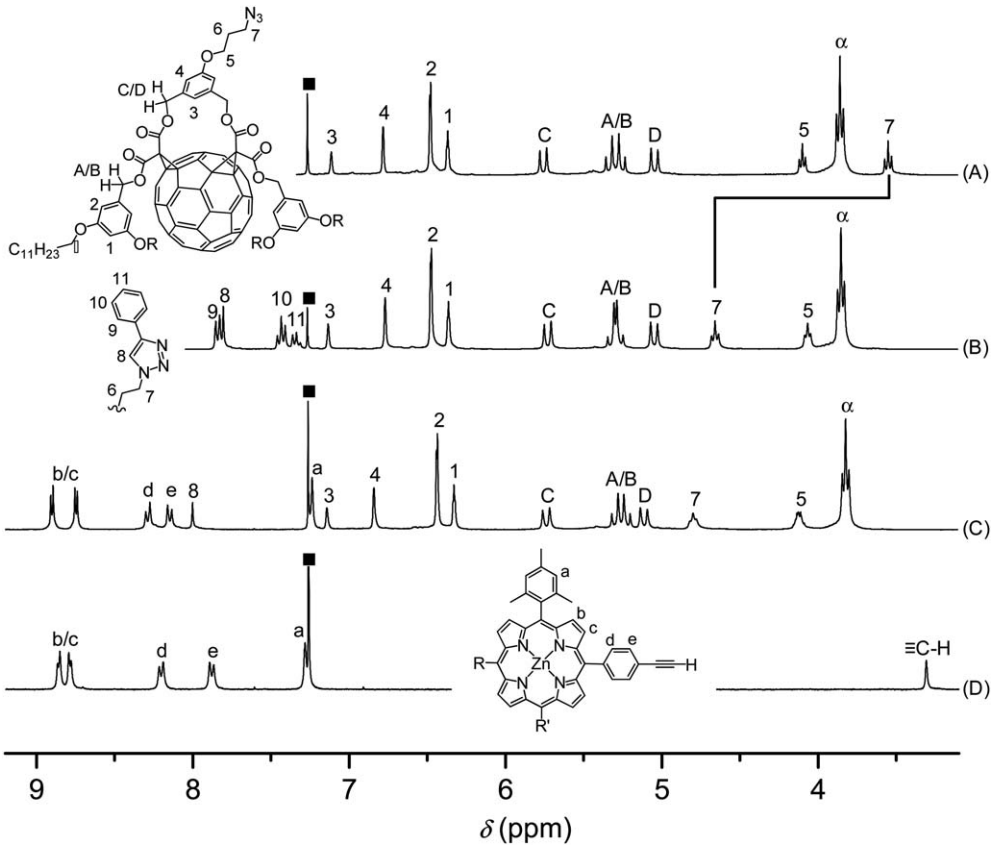

Fig. 1 ^{1}H NMR spectra ($CDCl_3$, 300 MHz) of compounds **7** (A), **F** (B), **F–P–F** (C) and **12** (D) (■ = solvent peak).

phenylacetylene in the presence of $CuSO_4 \cdot 5H_2O$ and sodium ascorbate in a mixture of CH_2Cl_2/H_2O (1/1) gave the clicked model compound **F** in 73% yield. As previously observed for click reactions with fullerene-based building blocks, azide cycloaddition on the C_{60} core does not significantly compete with the alkyne–azide click reaction leading to the 1,2,3-triazole derivatives. Compound **F** is highly soluble in common organic solvent and was thus easily characterized. The structure of compound **F** was confirmed by its ^{1}H and ^{13}C NMR spectra as well as by mass spectrometry. Inspection of the ^{1}H NMR spectrum clearly indicates the disappearance of the CH_2–azide (H-7) signal at $\delta = 3.55$ ppm (Fig. 1). Importantly, the ^{1}H NMR spectrum of **F** shows the typical singlet of the 1,2,3-triazole unit (H-8) at $\delta = 7.80$ ppm as well as the signal corresponding to the CH_2–triazole protons (H-7) at $\delta = 4.65$ ppm.

The synthesis of the porphyrin building block bearing two clickable terminal alkyne units (**12**) is depicted in Scheme 2. Compound **8**[23] and dipyrromethane **9**[24] were prepared according to previously reported methods. Porphyrin **10** was obtained by using the reaction conditions developed in the group of Lindsey.[25] The condensation of **8** and **9** was performed in $CHCl_3$ (commercial $CHCl_3$ containing 0.75% ethanol as stabilizer) at room temperature in the presence of $BF_3 \cdot Et_2O$. After 16 hours, *p*-chloranil (tetrachlorobenzoquinone) was added to irreversibly convert the porphyrinogen to the porphyrin. The desired tetraphenylporphyrin **10** was subsequently isolated in 23% yield. Metalation of **10** with $Zn(OAc)_2$ and treatment of the resulting **11** with TBAF gave compound **12**.

Treatment of **12** with fullerene azide **7** in the presence of $CuSO_4 \cdot 5H_2O$ and sodium ascorbate gave the targeted fullerene–porphyrin conjugate **F–P–F** in 64% yield. Inspection of the ^{1}H NMR spectrum of **F–P–F** (Fig. 1) clearly indicates the disappearance of the terminal alkyne units seen at $\delta = 3.31$ ppm in the starting building block (**12**) and the appearance of the typical signal of the 1,2,3-triazole units (H-8) at $\delta = 8.00$ ppm. As seen in the case of **F**, the diagnostic resonance corresponding to the CH_2–triazole protons (H-7) is observed at $\delta = 4.80$ ppm. The structure of **F–P–F** was also confirmed by mass spectrometry. As shown in Fig. 2, the MALDI-TOF mass spectrum of **F–P–F** displays a singly charged ion peak at $m/z = 4898.5$ corresponding to the expected molecular ion peak ($[M + H]^+$, calcd for $C_{332}H_{287}N_{10}O_{26}Zn$: 4898.36). Under our experimental conditions, only a very minor fragment is observed at $m/z = 4438.5$. The latter is ascribed to $[M - C_{31}H_{55}O_2]^+$ as a result of the cleavage of a 3,5-didodecyloxybenzylic ester subunit. It can be noted that this fragmentation is classically observed for such fullerene derivatives.[26] However, when compared to mass spectra recorded under much harsher FAB conditions, the fragmentation is very limited in the MALDI-TOF mass spectrum thus showing that the latter technique is an ideal tool for the characterization of such high molecular weight compounds.

The conformation adopted by compound **F–P–F** is an important issue for a better understanding of the photophysical properties. Indeed, the flexible linkers between the central porphyrin moiety and the two peripheral fullerene subunits may allow for either a fully extended or a folded conformation. The

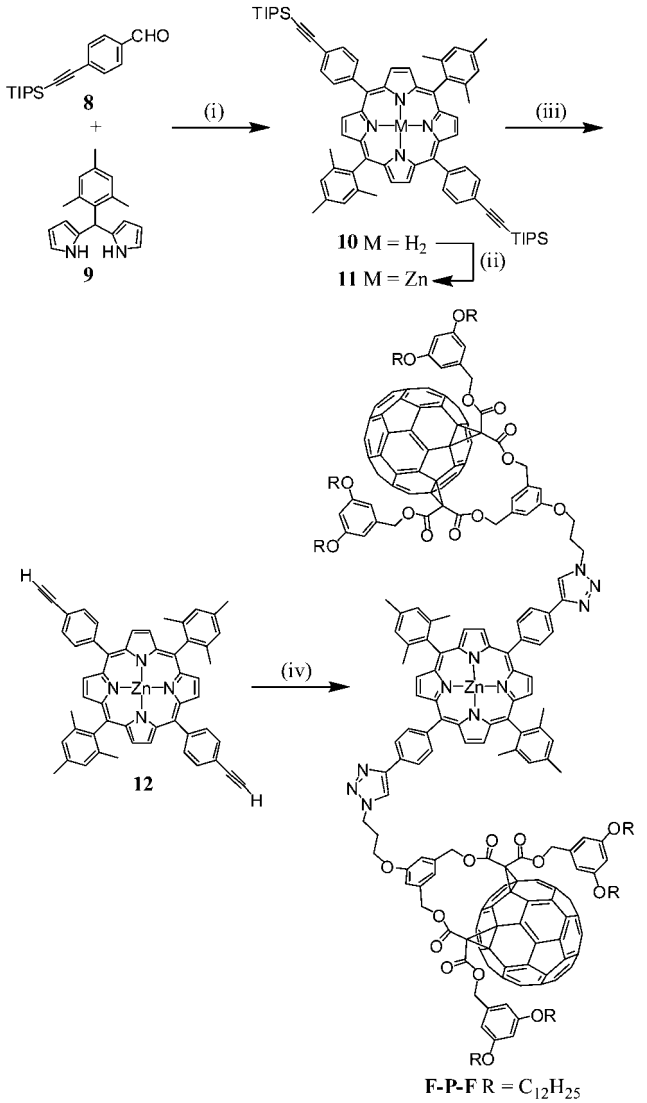

Scheme 2 *Reagents and conditions*: (i) $BF_3 \cdot Et_2O$, $CHCl_3$, rt, 16 h, then *p*-chloranil, Δ, 2 h (23%); (ii) $Zn(OAc)_2$, MeOH/$CHCl_3$, Δ, 2 h (95%); (iii) TBAF, THF, 0 °C, 2 h (94%); (iv) **7**, $CuSO_4 \cdot 5H_2O$, sodium ascorbate, CH_2Cl_2/H_2O, rt, 1 h (64%).

calculated structure of compound **F–P–F** depicted in Fig. 3 reveals that π-stacking interactions between the fullerene moieties and the central porphyrinic core take place in a folded conformation. Such attractive interactions between fullerenes and porphyrins have been already observed for several covalent and non-covalent C_{60}–porphyrin conjugates[5] and may contribute to stabilize the folded conformation in the case of **F–P–F**. This view is indeed supported by the 2D NOESY spectrum of **F–P–F** recorded in $CDCl_3$ at room temperature (Fig. S1†). Effectively, correlation peaks are observed between the 1,2,3-triazole proton (H-8) and both CH_2-5 and CH_2-7 groups of the propylene linker (see Fig. 1 for the numbering of the protons). The latter observation clearly reveals that CH_2-5 is spatially close to proton H-8. This is obviously possible only if compound **F–P–F** adopts a folded conformation. In the calculated structure, the distance between proton H-8 and its closest neighbor in the CH_2-5 unit is 3.29 Å for one 1,2,3-triazole ring and 4.36 Å for the other one in

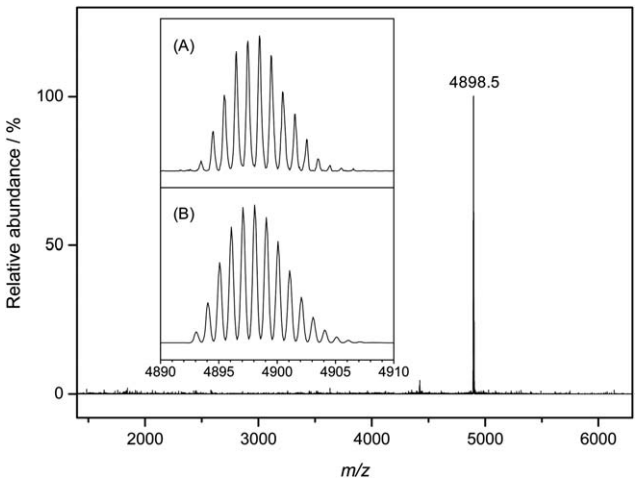

Fig. 2 MALDI-TOF mass spectrum of compound **F–P–F** recorded in the positive mode; the inset shows the observed (A) and the simulated (B) isotopic patterns of the pseudo-molecular ion peak ($[M + H]^+$, $C_{332}H_{287}N_{10}O_{26}Zn$).

perfect agreement with the observed NOE effects. Further correlation peaks observed between the protons of the mesityl groups (CH_3 and H-a) and some of the CH_2 moieties of the dodecyl chains are also consistent with a folded conformation. However, compound **F–P–F** being not a rigid molecule, this conclusion refers not to a fixed structure but to an energetically preferred conformation in this particular solvent ($CDCl_3$) resulting from attractive intramolecular fullerene–porphyrin interactions. It can be noted that the occurrence of such interactions is further supported by (i) the slight red-shift observed for the Soret band in the absorption spectrum of **F–P–F** when compared to model porphyrin **P**, and (ii) the observation of a NIR charge transfer emission upon photoexcitation in toluene (*vide infra*).

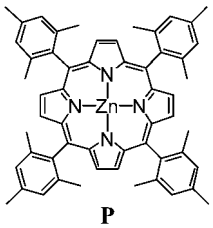

P

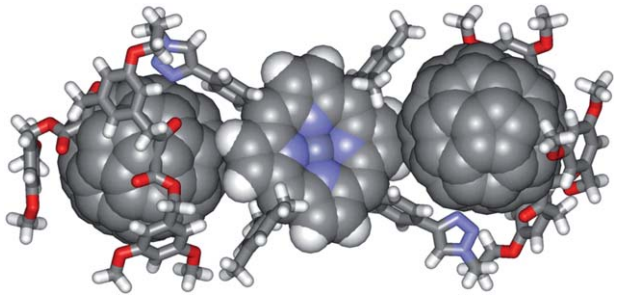

Fig. 3 Calculated structure of **F–P–F** (molecular modeling performed with *Spartan* at the PM3 level, the dodecyl chains have been replaced by methyl groups in the calculations).

Electrochemistry

The electrochemical properties of **F–P–F** were determined by cyclic voltammetry (CV) and Osteryoung Square Wave Voltammetry (OSWV). For the sake of comparison, electrochemical measurements have also been carried out with **F**, **12** and **P**. All the experiments were performed at room temperature in CH_2Cl_2 solutions containing tetra-*n*-butylammonium tetrafluoroborate (0.1 M) as supporting electrolyte and ferrocene (Fc) as internal reference, with a Pt wire as the working electrode and a saturated calomel electrode (SCE) as a reference. Potential data for all of the compounds are collected in Table 1. As typical examples, the cyclic voltammogram and the OSWVs (cathodic and anodic scans) of compound **F–P–F** are depicted in Fig. 4.

In the cathodic region, model compound **F** shows the classical behavior observed for fullerene *cis*-2 bis-adducts.[27] In addition to the observation of the three successive reductions of the fullerene unit, reduction peaks of electrogenerated products formed after the second reduction are also observed at −1.15 and −1.57 V *vs.* SCE (Fig. S2†). This specific behaviour of cyclopropanated fullerenes is most probably due to a bond breaking in the cyclopropane ring, known as the retro-Bingel reaction.[28] In the anodic region, model compound **F** shows two irreversible peaks which can be likely attributed to the oxidation of the dialkyloxyphenyl and/or 4-phenyl-1,2,3-triazol units.[29] Model compounds **12** and **P** display the characteristic electrochemical behaviour of Zn(II)–porphyrin derivatives[30] with two quasi-reversible porphyrin-centered one-electron transfer processes in both the cathodic and the anodic regions (Fig. S3†). The voltammograms recorded for hybrid compound **F–P–F** show the characteristic electrochemical features of both constitutive units, *i.e.* fullerene and Zn(II)–porphyrin. The comparison of the redox potentials of **F–P–F** with the corresponding model compounds clearly shows that the two first reduction waves correspond to fullerene-centered processes, while the two first oxidation processes are centered on the porphyrin core. The third reduction peak is ascribed to the electrogenerated products formed after the second reduction as observed in the case of **F**. The fourth reduction process probably contains contributions from both C_{60} and porphyrin moieties. Finally, the fifth peak corresponds most likely to a fullerene-centered reduction. As shown in Fig. 4, the two fullerene subunits behave as independent redox centers and the relative intensity of the first fullerene-reduction relative to the first porphyrin-based oxidation is in the expected 2 : 1 ratio. Comparison of the redox potentials values of **F–P–F** with those of the corresponding model compounds **F** and **P** reveals

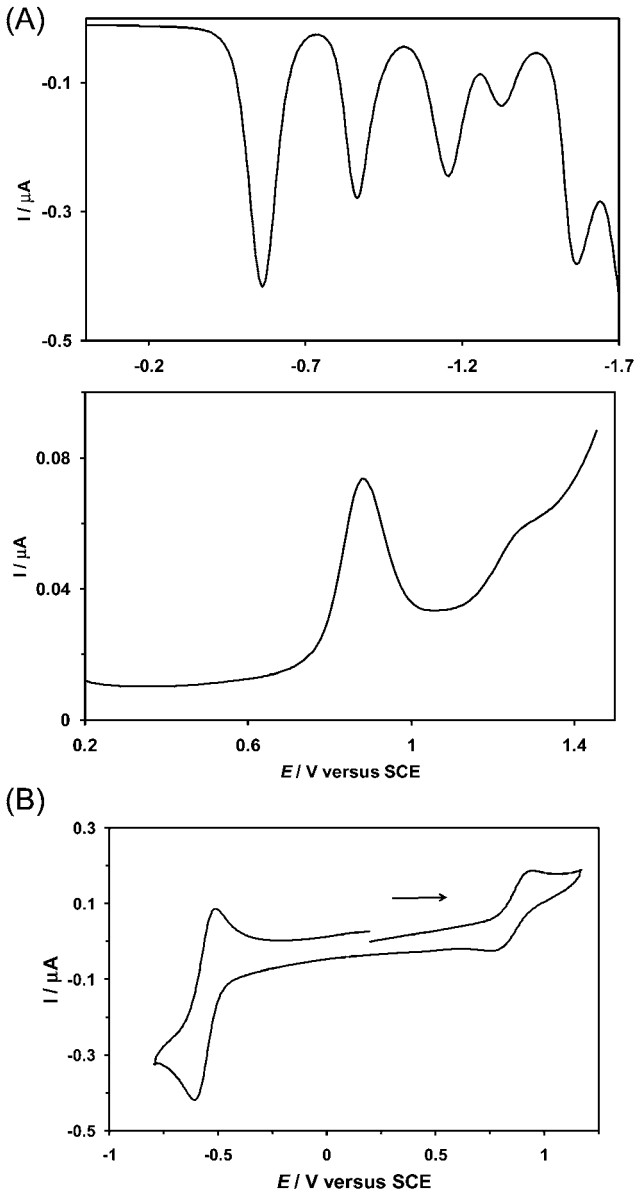

Fig. 4 (A) OSWVs (top: cathodic scan; bottom: anodic scan) of compound **F–P–F** on a Pt electrode in CH_2Cl_2 + 0.1 M *n*-Bu_4NBF_4 at room temperature. (B) Cyclic voltammogram of compound **F–P–F** on a Pt electrode at $v = 0.1$ V s^{-1} in CH_2Cl_2 + 0.1 M *n*-Bu_4NBF_4.

Table 1 Electrochemical data of **F**, **P**, **12** and **F–P–F** determined by OSWV on a Pt working electrode in CH_2Cl_2 + 0.1 M *n*-Bu_4NBF_4 at room temperature in the presence of ferrocene used as internal reference[ab]

	Oxidation			Reduction				
	E_3	E_2	E_1	E_1	E_2	E_3	E_4	E_5
F		+1.97	+1.69	−0.55	−0.87	−1.15[c]	−1.35	−1.57[c]
12		+1.19	+0.91	−1.31	−1.71			
P		+1.20	+0.86	−1.40	−1.62			
F–P–F	+1.76	+1.26	+0.88	−0.56	−0.86	−1.15[c]	−1.33	−1.56[c]

[a] OSWVs were obtained using a sweep width of 20 mV, a frequency of 10 Hz, and a step potential of 5 mV. [b] Values in V *vs.* SCE (Fc^+/Fc is observed at +0.55 ± 0.01 V *vs.* SCE). [c] Waves corresponding to an electrogenerated species obtained after the second fullerene-centered reduction step.

only a minor influence of the fullerene subunits on the porphyrin moiety and *vice versa*. This observation, however, does not indicate the absence of intramolecular fullerene–porphyrin interactions (*vide supra*). Effectively, redox potentials of fullerene–donor conjugates are generally very weakly affected by intramolecular π–π interactions even in cyclic systems in which the two components are forced to be at the van der Waals contact.[31]

Ground state absorption and luminescence properties

The electronic absorption spectra of model compounds **F** and **P**, and fullerene–porphyrin conjugate **F–P–F** in toluene are shown in Fig. 5. Below 390 nm, the fullerene absorption is stronger than that of the porphyrin, whereas in the visible spectral region an opposite pattern is observed. The spectrum of **P** is quite similar to that of Zn(II) *meso*-tetraphenylporphyrin (ZnTPP).[32] This is an expected result since the side group on the *meso*-phenyl rings does not affect much the delocalization of the porphyrin π-systems. The maximum of the Soret band, corresponding to the transition to the second singlet excited state, is located at 424 nm ($\varepsilon = 521\,000\ M^{-1}\ cm^{-1}$) in toluene.

In the UV region, the absorption spectrum of **F–P–F** exhibits minor differences when compared with the sum of the spectra of the corresponding model compounds. In contrast, significant differences can be observed in the Vis region. In particular, a slight red-shift ($\lambda_{max} = 426$ nm) as well as an intensity decrease of the Soret band ($\varepsilon = 434\,000\ M^{-1}\ cm^{-1}$) are observed. This may suggest some interactions between at least one of two fullerenes with the porphyrin macrocycle. This kind of behavior has been typically found in systems with a face-to-face porphyrin–fullerene interchromophoric arrangement.[1f] Compared to the algebraic sum of the components, **F–P–F** also exhibits a concentration-independent weak tail of the absorption profile above 650 nm, which is a further clue for ground state charge transfer interaction between the two chromophores, in line with previous reports (Fig. 5).[7]

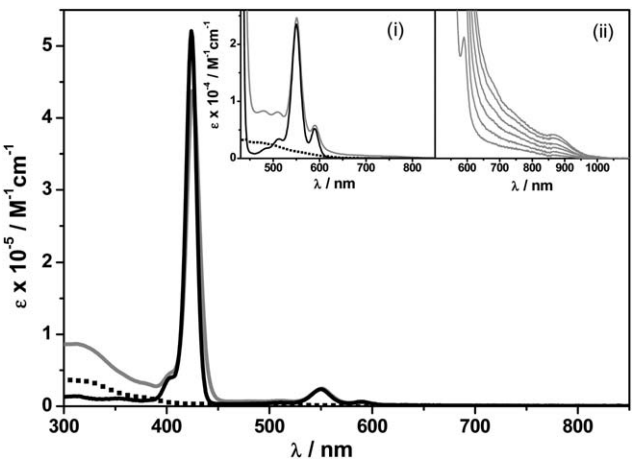

Fig. 5 Absorption spectra of **F–P–F** (grey), **F** (dotted black), and **P** (black) in toluene solution at 298 K; insets (i) zoom of Q band region and (ii) absorption spectra of **F–P–F** in NIR region at various concentrations ([**F–P–F**] = 7.4–46 μM).

The most relevant luminescence data for all the investigated compounds are reported in Table 2, where the emission maxima refer to the spectra corrected for the detector response.

In toluene solution at room temperature, **P** exhibits a fluorescence band ($\lambda_{max} = 645$ nm, $\tau_S = 2.1$ ns, $\Phi_{fl} = 2.4\%$); at 77 K both fluorescence and phosphorescence are detected (Table 2 and Fig. 6). The porphyrin fluorescence intensity of **F–P–F** is quenched by about 75% when compared to **P** at 298 K (Table 2), and the lifetime is accordingly reduced from 2.1 to 1.0 ns, corresponding to a quenching rate constant of $5.2 \times 10^8\ s^{-1}$. The quenching process can be attributed to singlet energy transfer to the fullerene moiety, in line with literature reports for analogous multichromophoric fullerene–porphyrin systems in apolar media;[3] this hypothesis will be verified in the next sections. In **F–P–F** the porphyrin quenching turns out to be relatively slow compared to previously investigated similar arrays due to the long through bond distance between the energy donor and acceptor, assuming an extended conformation. Also a weak phosphorescence signal (quenched by about 65%) is still observable for **F–P–F** ($\lambda_{max} = 775$ nm, $\tau_T = 20$ ms) at 77 K. The typical weak fluorescence band is observed for the bismethanofullerene reference compound **F** ($\lambda_{max} = 700$ nm, $\tau_S = 1.6$ ns). This band cannot be observed in **F–P–F** because of the spectral overlapping with the residual porphyrin emission, still much more intense, even when excitation is addressed mainly to the fullerene moiety ($\lambda_{exc} = 380$ nm).

In benzonitrile solution at room temperature, the porphyrin fluorescence is quenched to a similar extent as in toluene, both in intensity and lifetime (Table 2), also suggesting a relatively slow quenching process, as found in toluene. Interestingly, the porphyrin phosphorescence at low temperature in this solvent could not be detected for **F–P–F**.

Table 2 Luminescence data in toluene and benzonitrile

	Toluene					Benzonitrile				
	298 K			77 K		298 K			77 K	
Compound	$\lambda_{max}{}^a$/nm	τ/ns	Φ_{em} (%)	$\lambda_{max}{}^a$/nm	$\lambda_{max}{}^b$/nm	$\lambda_{max}{}^a$/nm	τ/ns	Φ_{em} (%)	$\lambda_{max}{}^a$/nm	$\lambda_{max}{}^b$/nm
F	700	1.6	~0.01			700	1.5	~0.01		
P	645	2.1	2.4	602	784	606	1.9	2.9	607	800
F–P–F	645	1.0	0.60	597	775	609	1.1	1.0	607	—[c]

[a] Fluorescence: from corrected emission spectra. [b] Phosphorescence. [c] Not detected.

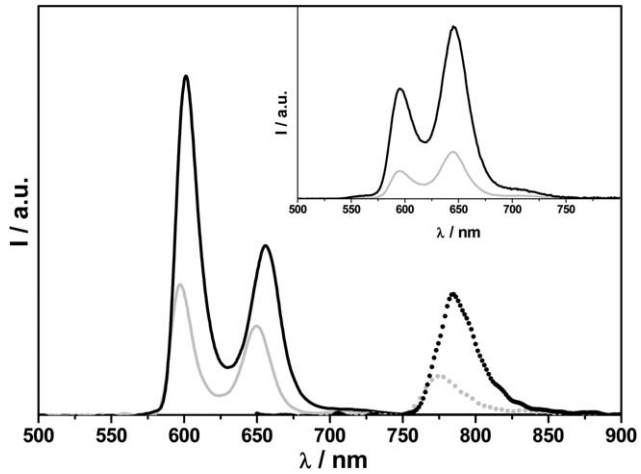

Fig. 6 Corrected emission spectra of **F–P–F** (fluorescence: grey, phosphorescence: dotted grey) and **P** (fluorescence: black, phosphorescence: dotted black) in toluene solution at 77 K. Inset: fluorescence at 298 K.

Singlet oxygen sensitization and NIR emission

In order to trace the formation of porphyrin and/or fullerene triplets,[26a] we measured the sensitized singlet oxygen ($^1O_2$*) luminescence at 1270 nm in toluene (Fig. S4†).[33] Setting *meso*-tetraphenylporphyrin (TPP) as standard, which displays a singlet oxygen sensitization yield (Φ_Δ) equal to 0.70[34] in toluene solution, we measured values of 0.70 for **P**, 0.60 for **F** and 0.45 for **F–P–F**. The formation of singlet oxygen in **F–P–F** is in line with the finding of extensive formation of fullerene triplet in toluene by transient absorption spectroscopy (*vide infra*). By contrast, no sensitized $^1O_2$* luminescence is detected in benzonitrile solution by exciting **F–P–F** (Fig. S4†). This suggests that different photoinduced processes occur in the multicomponent array in the two solvents, as it will be evidenced by transient absorption studies.

Interestingly, **F–P–F** exhibits a weak and broad emission band centered at *ca.* 950 nm in toluene solution (Fig. 7); its faint intensity prevented the determination of the lifetime. In analogy with previous findings in face-to-face porphyrin–fullerene systems[1f,7] this band is attributed to an emitting charge transfer state that can be generated by a minority of **F–P–F** systems, in the frame of a dynamic equilibrium, in which the two chromophores are in a close edge-to-face conformation. The excitation spectrum of **F–P–F** taken at 950 nm showed the typical spectral features of a porphyrin moiety, and particularly the diagnostic Soret band at *ca.* 420 nm and Q bands at 550 nm. This rules out that the observed NIR band is due to exciplex emission and suggests that the porphyrin excited states are partly deactivated to a low-lying CT level. The fact that the absorption tail above 650 nm (ε = 375 M^{-1} cm^{-1}) is weaker than those previously observed[1f,7] suggests that only a minor fraction of molecules are involved in the edge-to-face interactions, contrary to what happened in face-to-face systems where molecules engaged in CT interactions are the large majority.[7a] In benzonitrile solution, under steady state irradiation at the porphyrin Q bands, no NIR emission such as that in Fig. 7 is detected for **F–P–F**. This is not surprising since CT luminescence has never been observed previously for face-to-face systems in this solvent, due to the energy gap law (lower CT energy, faster nonradiative deactivation rates) or to the fact that the charge recombination (CR) process of the porphyrin–fullerene pairs is highly exergonic and lies in the Marcus inverted region.[1f] Under this regime, CR processes are expected to be faster in more polar media (*i.e.* benzonitrile *vs.* toluene), owing to a decrease of the activation energy for charge recombination.[35]

In summary, **F–P–F** shows clear evidence of interchromophoric excited state interactions. The porphyrin centered fluorescence is quenched, while a new CT emission band in the near infrared spectral region is recorded in toluene solution. However, the main deactivation pathway in apolar toluene leads to the formation of the fullerene triplet, which most likely occurs through porphyrin → fullerene singlet energy transfer, followed by regular intersystem crossing within the carbon sphere, as observed in many fullerene dyads.[26a]

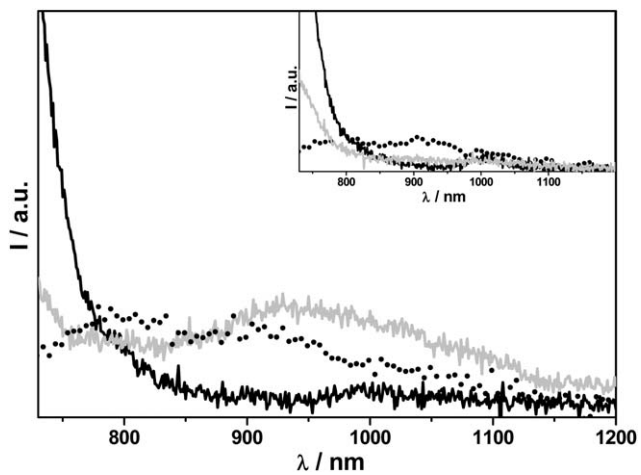

Fig. 7 Emission spectra in the near infrared spectral region at 298 K in toluene of **F–P–F** (grey), **F** (dotted black) and **P** (black) upon excitation at 550 nm, A = 0.300. Inset: in benzonitrile.

Transient absorption spectroscopy

The nanosecond transient absorption spectrum of **P** (Fig. S5†) shows the typical zinc porphyrin triplet absorption spectra (λ_{max} = 460 nm); its lifetime is 177 and 130 μs in deoxygenated benzonitrile and toluene solutions, respectively. The nanosecond transient absorption spectrum of **F** in benzonitrile (Fig. S5†) shows the characteristic triplet–triplet absorption band (λ_{max} = 720 nm).[36] A first order decay with a lifetime of 24 μs is found, which corresponds to the non-radiative $T_1 \rightarrow S_0$ deactivation process of **F**.

The shape of the nanosecond transient absorption spectrum of **F–P–F** in benzonitrile (Fig. 8) is very different from that of its model compounds. Immediately after excitation of **F–P–F** with 560 nm laser pulse, where the porphyrin component is selectively excited with a ratio of about 10 : 1 with respect to fullerene, the bleaching of the ground state porphyrin Q-bands at 550 and 600 nm and an intense absorption of the porphyrin triplet at 470 nm are recorded. With an increase of delay time, spectral changes in the absorptions at *ca.* 650 and 1005 nm arise and decay simultaneously with τ = 0.48 μs (Fig. 8). We assign the absorption

band around 650 nm to zinc porphyrin radical cation ($ZnP^{\bullet+}$)[37] and that around 1005 nm to the bismethanofullerene radical anion ($C_{60}^{\bullet-}$),[38] respectively. The identical lifetimes, within the experimental uncertainty, indicate that the same species is monitored, namely the charge separated state. The rise time of the charge separated state is about 20 ns, which rules out the role of the singlet levels as reacting species and indicates that the ion pair is formed by the fullerene triplet. This is fully reasonable on the basis of the electrochemical data, which indicate that the energy of the charge separated state is 1.44 eV in CH_2Cl_2, and must be somewhat lower in more polar benzonitrile, which is compatible with a triplet energy of bismethanofullerenes of 1.40 eV.[26a] Indeed the porphyrin centred triplet state is detected at around 480 nm in **F–P–F**, which decays with $\tau \approx 30$ ns; this suggests some residual electron transfer from the porphyrin centered triplet state, populated *via* intersystem crossing. The absence of formation of long-lived triplet species either in the porphyrin or the fullerene chromophores, is verified by the absence of sensitized singlet oxygen luminescence at 1270 nm in air equilibrated benzonitrile solution (see ESI†) as well as by the lack of phosphorescence at 77 K (*vide supra*).

For **F–P–F** in toluene, no charge separated state is detected in the nanosecond regime (Fig. 8). In a timescale below our experimental resolution, *i.e.* less than 10 ns, the growth of the fullerene triplet is detected at 720 nm, upon excitation of the porphyrin moiety. This dynamics is compatible with the quenching of the porphyrin singlet detected *via* fluorescence spectroscopy ($k = 5.2 \times 10^8$ s^{-1}, see above). The fact that (i) the quenched porphyrin singlet lifetimes are identical in toluene and benzonitrile, despite a completely different excited state reactivity and (ii) singlet levels do not feed electron transfer in benzonitrile are robust clues for porphyrin → fullerene singlet energy transfer in both media as the primary photoinduced event.

The fullerene triplet lifetime is 3.8 and 0.34 μs in deoxygenated and air-equilibrated solution, respectively. Interestingly, the fullerene triplet lifetime of **F–P–F** (3.8 μs) is significantly reduced relative to that of the model fullerene **F** (20 μs) in oxygen-free solution. This suggests that a dynamic quenching of the long lived fullerene triplet states in **F–P–F** occurs, with a rate constant of 2.1×10^5 s^{-1}. This could be a consequence of a dynamic equilibrium that, on the microsecond timescale, would allow the deactivation of the fullerene triplet states in **F–P–F** with an extended conformation (majority) to the lower-lying CT species (minority).[7a] To further strengthen the hypothesis of such a dynamic equilibrium between compact and extended conformations, it can be noted that the Φ_Δ value of **F–P–F** (0.45) is slightly smaller than that of **F** (0.60), again suggesting the presence of a minority of CT states that are known to be incapable of sensitizing the formation of $^1O_2$*.[35]

The photoinduced intramolecular processes evidenced for **F–P–F** in both solvents (toluene and benzonitrile) can be summarized as follows. In toluene, no long lived charge separated state could be detected by nanosecond transient absorption spectroscopy. On the other hand, efficient singlet energy transfer from the porphyrin to the fullerene excited states followed by population of the fullerene triplet level is evidenced by time resolved absorption and luminescence experiments. The triplet state character of the observed excited state was further confirmed by the singlet oxygen sensitization measurements. Moreover, a porphyrin–fullerene charge transfer interaction was evidenced by a broad and weak emission band at around 940 nm. This kind of interaction can only be set up through very tight porphyrin/fullerene pair configurations, which, in the present case can be

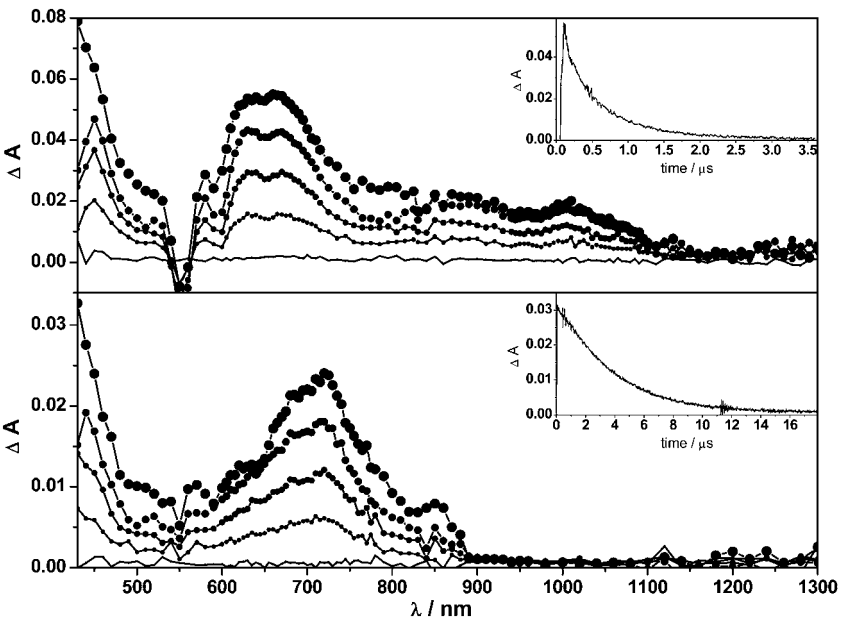

Fig. 8 Top: transient absorption spectra of **F–P–F** ($A = 0.350$) in oxygen-free benzonitrile. Depicted spectral traces are at 0.1, 0.16, 0.34, 0.70, 2.5 μs (from bigger to smaller circles) after the laser pulse. Inset: absorption decay at 650 nm. $\lambda_{exc} = 560$ nm. Energy: 1.0 mJ per pulse. Bottom: transient absorption spectra of **F–P–F** ($A = 0.350$) in oxygen-free toluene. Depicted spectral traces are at 0.1, 1.2, 2.8, 5.3, 16 μs (from bigger to smaller circles) after the laser pulse. Inset: absorption decay at 720 nm. $\lambda_{exc} = 560$ nm. Energy: 2.0 mJ per pulse.

only face-to-edge and not face-to-face as observed previously.[1f] This species is present only as a minor fraction, in the frame of a dynamic equilibrium. The quenching of the fullerene centred triplet state in **F–P–F** in oxygen free solution is also a good indication of this hypothesis. In benzonitrile, no emission in the NIR region could be detected, but photoinduced electron transfer was unambiguously evidenced, since the free-radical ions $P^{\bullet+}$ and $F^{\bullet-}$ were identified by flash spectroscopy.

Conclusions

In conclusion, we have developed a stable C_{60} derivative bearing an azide functional group allowing its further functionalization by reaction with terminal alkynes under the copper mediated Huisgen 1,3-dipolar cycloaddition conditions. This building block has been used for the preparation of fullerene–porphyrin conjugate **F–P–F** by reaction with a Zn(II)–porphyrin bearing two terminal alkyne units. Molecular modeling and 2D NOESY experiments on the resulting hybrid system have revealed a folded conformation stabilized by intramolecular π-stacking interactions between the fullerene moieties and the central porphyrinic core. The electrochemical properties of hybrid compound **F–P–F** have been investigated. Whereas the first reduction is centered on the C_{60} unit, the oxidation is centered on the porphyrin moiety. Photophysical studies revealed strong excited state interactions between the different components in **F–P–F**. Indeed, intramolecular photoinduced processes have been evidenced by steady-state fluorescence spectroscopy and time-resolved absorption and luminescence techniques. In a polar solvent such as benzonitrile, **F–P–F** undergoes an efficient photoinduced electron transfer from both fullerene and porphyrin triplet levels. The resulting charge separated state is relatively long lived ($\tau = 0.48$ μs). In contrast, intramolecular energy transfer has been evidenced in apolar toluene. Interestingly, a conformational equilibrium allowing an intramolecular porphyrin–fullerene π–π interaction is responsible for the dynamic quenching of the fullerene centered triplet state that populates a CT state from which a NIR emission could be detected.

Experimental

Materials and methods

All reagents were used as purchased from commercial sources without further purification. Compounds **1**,[16] **2**,[17] **5**,[18] **8**[23] and **9**[24] were prepared according to previously reported procedures. Solvents were dried using standard techniques prior to use. All reactions were performed in standard glassware. Evaporation was done using water aspirator and drying *in vacuo* at 10^{-2} Torr. Column chromatography: silica gel 60 (230–400 mesh, 0.040–0.063 mm) was purchased from E. Merck. TLC: precoated glass sheets with silica gel 60 F_{254} (Merck), visualization by UV light. Gel permeation chromatography was performed on Biorad, Biobeads SX-1 under the use of CH_2Cl_2 as eluent. NMR spectra were recorded on a Bruker AM 300 (300 MHz) with solvent signal as reference. MALDI-TOF-MS were obtained on a Bruker ULTRAFLEX TOF/TOF mass spectrometer with a dithranol matrix. Elemental analysis was performed by the analytical service at the Laboratoire de Chimie de Coordination (Toulouse, France).

Synthesis

Compound 3. A mixture of **1** (1.51 g, 5.93 mmol), **2** (2.27 g, 5.93 mmol), K_2CO_3 (2.05 g, 14.82 mmol) and LiBr (0.26 g, 2.96 mmol) in dry DMF (10 mL) was stirred at 80 °C for 96 h. The mixture was cooled to room temperature, filtered and evaporated. Column chromatography (SiO_2, cyclohexane/CH_2Cl_2 8/2) gave **3** (0.92 g, 33%) as a colorless oil. IR (neat): 2097 ($-N_3$). ^{1}H NMR ($CDCl_3$, 300 MHz): 0.12 (s, 12H), 0.96 (s, 18H), 2.06 (m, 2H), 3.52 (t, $J = 6$ Hz, 2H), 4.06 (t, $J = 6$ Hz, 2H), 4.72 (s, 4H), 6.78 (m, 2H), 6.88 (m, 1H). ^{13}C NMR ($CDCl_3$, 75 MHz): δ −5.1, 18.6, 26.1, 28.9, 48.5, 64.5, 65.0, 110.8, 116.2, 143.2, 158.9.

Compound 4. A 1 M solution of Bu_4NF in THF (3.8 mL, 3.80 mmol) was added to a solution of **3** (810 mg, 1.74 mmol) in dry THF (50 mL) at 0 °C. After 1 h, the mixture was allowed to warm to room temperature, then stirred for 2 h and poured into water. The organic layer was diluted with CH_2Cl_2, washed with water, dried ($MgSO_4$), filtered and concentrated. Column chromatography (SiO_2, CH_2Cl_2/MeOH 97/3) gave **4** (300 mg, 73%) as a colorless oil. IR (neat): 3327 (O–H), 2094 ($-N_3$). ^{1}H NMR ($CDCl_3$, 300 MHz): 2.00 (m, 2H), 3.46 (t, $J = 6$ Hz, 2H), 3.99 (t, $J = 6$ Hz, 2H), 4.51 (s, 4H), 6.74 (m, 2H), 6.84 (m, 1H).

Compound 6. DCC (645 mg, 3.16 mmol) was added to a solution of **4** (300 mg, 1.26 mmol), **5** (1.78 g, 3.16 mmol), HOBt (cat) and DMAP (61 mg, 0.50 mmol) in CH_2Cl_2 (50 mL) at 0 °C. After 1 h, the mixture was allowed to warm slowly to room temperature, then stirred for 72 h, filtered, and evaporated. Column chromatography (SiO_2, CH_2Cl_2/cyclohexane 9/1) gave **6** (1.09 mg, 65%) as a colorless oil. IR (neat): ν 2097 ($-N_3$), 1736 (C=O). ^{1}H NMR ($CDCl_3$, 300 MHz): 0.89 (t, $J = 7$ Hz, 12H), 1.20–1.45 (m, 72H), 1.76 (m, 8H), 2.03 (m, 2H), 3.50 (m, 6H), 3.91 (t, $J = 7$ Hz, 8H), 4.03 (t, $J = 6$ Hz, 2H), 5.10 (s, 4H), 5.14 (s, 4H), 6.41 (t, $J = 2$ Hz, 2H), 6.46 (d, $J = 2$ Hz, 4H), 6.86 (m, 2H), 6.91 (m, 1H). ^{13}C NMR ($CDCl_3$, 75 MHz): δ 14.2, 22.8, 26.2, 28.8, 29.3, 29.4, 29.5, 29.6, 29.7, 29.75, 29.8, 32.0, 41.5, 48.3, 64.7, 66.8, 67.3, 68.2, 101.2, 106.5, 114.1, 120.1, 137.3, 137.3, 159.2, 160.6, 166.2, 166.3. Anal. Calcd for $C_{79}H_{127}N_3O_{13}$: C 71.51, H 9.65, N 3.17; found: C 71.48, H 9.55, N 3.14%.

Compound 7. DBU (0.26 mL, 1.70 mmol) was added to a stirred solution of C_{60} (267 mg, 0.37 mmol), I_2 (235 mg, 0.93 mmol) and **6** (492 mg, 0.37 mmol) in toluene (550 mL) at room temperature. The resulting solution was stirred for 12 h, then filtered through a short plug of SiO_2 (CH_2Cl_2) and concentrated. Column chromatography (SiO_2, CH_2Cl_2/hexane 45/55) followed by gel permeation chromatography (Biobeads SX-1 CH_2Cl_2) gave **7** (430 mg, 56%) as a dark-red glassy product. IR (neat): 2096 ($-N_3$), 1748 (C=O). UV/Vis (CH_2Cl_2): 256 (91 500), 319 (35 200), 378 (13 470), 437 (3200), 466 (sh, 3000). ^{1}H NMR ($CDCl_3$, 300 MHz): 0.89 (t, $J = 7$ Hz, 12H), 1.20–1.45 (m, 72H), 1.72 (m, 8H), 2.08 (m, 2H), 3.55 (t, $J = 6$ Hz, 2H), 3.85 (t, $J = 7$ Hz, 8H), 4.09 (t, $J = 6$ Hz, 2H), 5.04 (d, $J = 13$ Hz, 2H), 5.29 (d, $J = 12$ Hz, 2H), 5.75 (d, $J = 13$ Hz, 2H), 6.36 (t, $J = 2$ Hz, 2H), 6.47 (d, $J = 2$ Hz, 4H), 6.78 (m, 2H), 7.11 (m, 1H). ^{13}C NMR ($CDCl_3$,

75 MHz): 14.3, 22.8, 26.3, 28.9, 29.4, 29.5, 29.6, 29.8, 29.85, 29.9, 31.1, 31.6, 32.1, 48.3, 49.2, 64.8, 67.0, 67.4, 68.3, 68.8, 70.7, 101.8, 107.3, 112.6, 115.6, 134.6, 135.9, 136.3, 136.7, 138.0, 138.4, 140.2, 141.2, 141.3, 142.4, 142.9, 143.3, 143.7, 143.9, 144.1, 144.3, 144.5, 144.7, 145.1, 145.2, 145.3, 145.5, 145.7, 145.85, 145.9, 146.2, 147.5, 147.6, 147.65, 148.8, 158.9, 160.6, 162.7. MALDI-MS: 2042.8 ([MH]$^+$, calcd for $C_{139}H_{124}N_3O_{13}$: 2042.91).

Compound F. $CuSO_4 \cdot 5H_2O$ (1 mg, 0.006 mmol) was added to a mixture of **7** (90 mg, 0.044 mmol), phenylacetylene (10 mg, 0.098 mmol) and sodium ascorbate (4 mg, 0.02 mmol) in CH_2Cl_2/H_2O (1/1, 2 mL) at room temperature. The mixture was stirred for 16 h. The organic layer was diluted with CH_2Cl_2, washed with water, dried over $MgSO_4$, filtered and concentrated. Column chromatography (SiO_2, CH_2Cl_2/cyclohexane 9/1) gave **F** (70 mg, 73%) as a dark red glassy product. IR (neat): 1748 (C=O). ^{1}H NMR ($CDCl_3$, 300 MHz): 0.89 (t, $J = 7$ Hz, 12H), 1.20–1.45 (m, 72H), 1.72 (m, 8H), 2.48 (m, 2H), 3.85 (t, $J = 7$ Hz, 8H), 4.06 (t, $J = 6.5$ Hz, 2H), 4.65 (t, $J = 6$ Hz, 2H), 5.04 (d, $J = 13$ Hz, 2H), 5.29 (d, $J = 12$ Hz, 2H), 5.72 (d, $J = 13$ Hz, 2H), 6.36 (t, $J = 2$ Hz, 2H), 6.47 (d, $J = 2$ Hz, 4H), 6.76 (m, 2H), 7.13 (m, 1H), 7.33 (m, 1H), 7.43 (m, 2H), 7.80 (s, 1H), 7.83 (d, $J = 8$ Hz, 2H). ^{13}C NMR ($CDCl_3$, 75 MHz): 14.3, 22.8, 26.2, 29.4, 29.5, 29.6, 29.7, 29.75, 29.8, 29.9, 30.1, 32.0, 47.3, 49.2, 64.4, 66.9, 67.3, 68.2, 68.8, 70.7, 101.8, 107.3, 112.5, 115.7, 120.2, 125.8, 128.3, 128.9, 130.6, 134.5, 135.9, 136.2, 136.6, 137.9, 138.5, 140.1, 141.2, 141.3, 142.4, 142.8, 143.3, 143.7, 143.8, 144.1, 144.2, 144.4, 144.7, 145.1, 145.2, 145.3, 145.3, 145.4, 145.7, 145.8, 146.2, 147.4, 147.5, 147.6, 147.9, 148.7, 158.6, 160.5, 162.7. Anal. Calcd for $C_{147}H_{129}N_3O_{13}.H_2O$: C 81.60, H 6.10, N 1.94; found: C 81.53, H 6.11, N 1.91%. MALDI-MS: 2146 ([M]$^+$, calcd for $C_{147}H_{139}N_3O_{13}$: 2145.65).

Compound 10. A 0.8 M solution of $BF_3 \cdot Et_2O$ in $CHCl_3$ (1.3 mL, 1.04 mmol) was added to a stirred solution of **8** (1 g, 3.49 mmol) and **9** (0.92 g, 3.49 mmol) in $CHCl_3$ (containing 0.75% EtOH, 350 mL) at room temperature. After 16 h, *p*-chloranil (2.57 g, 10.47 mmol) was added. The resulting solution was heated under reflux for 2 h and concentrated. Two successive column chromatographic separations (SiO_2, CH_2Cl_2/cyclohexane 6/4 to 6/3) gave **10** (421 mg, 23%) as a purple solid. IR (neat): 2153 (C≡C). UV/Vis (CH_2Cl_2): 420 (437 000), 515 (39 700), 550 (26 500), 591 (26 500), 647 (265 000). ^{1}H NMR ($CDCl_3$, 300 MHz): −2.61 (s, 2H), 1.27 (m, 42H), 1.85 (s, 12H), 2.65 (s, 6H), 7.30 (s, 4H), 7.88 (d, $J = 8$ Hz, 4H), 8.19 (d, $J = 8$ Hz, 4H), 8.71 (d, $J = 5$ Hz, 4H), 8.71 (d, $J = 5$ Hz, 4H).

Compound 11. A solution of $Zn(OAc)_2 \cdot 2H_2O$ (764 mg, 3.5 mmol) in methanol (4 mL) was added to a solution of **10** (370 mg, 0.35 mmol) in $CHCl_3$ (40 mL) at room temperature. The resulting solution was stirred for 2 h. The organic layer was diluted with $CHCl_3$, washed with water, dried (Na_2SO_4), filtered and concentrated. Column chromatography (SiO_2, cyclohexane/CH_2Cl_2/Et_3N 80/19/1) gave **11** (372 mg, 95%) as a purple solid. IR (neat): 2153 (C≡C). UV/Vis (CH_2Cl_2): 421 (700 000), 549 (52 800), 589 (26 400), 591 (26 500). ^{1}H NMR ($CDCl_3$, 300 MHz): 1.28 (m, 42H), 1.84 (s, 12H), 2.65 (s, 6H), 7.30 (s, 4H), 7.89 (d, $J = 8$ Hz, 4H), 8.21 (d, $J = 8$ Hz, 4H), 8.80 (d, $J = 5$ Hz, 4H), 8.90 (d, $J = 5$ Hz, 4H).

Compound 12. A 1 M solution of TBAF in THF (0.4 mL, 0.4 mmol) was added to a solution of **11** (227 mg, 0.20 mmol) in THF (20 mL) at 0 °C. After 1 h, the mixture was allowed to warm to room temperature, then stirred for 1 h and poured into water. The organic layer was diluted with CH_2Cl_2, washed with water, dried (Na_2SO_4), filtered and concentrated. Column chromatography (SiO_2, CH_2Cl_2/cyclohexane 3/7) gave **12** (153 mg, 94%) as a purple solid. IR (neat): 3294 (≡C–H), 2150 (C≡C). ^{1}H NMR ($CDCl_3$, 300 MHz): 1.82 (s, 12H), 2.63 (s, 6H), 3.31 (s, 2H), 7.28 (s, 4H), 7.88 (d, $J = 8$ Hz, 4H), 8.20 (d, $J = 8$ Hz, 4H), 8.79 (d, $J = 5$ Hz, 4H), 8.86 (d, $J = 5$ Hz, 4H).

Compound F–P–F. $CuSO_4 \cdot 5H_2O$ (0.5 mg, 0.003 mmol) was added to a mixture of **7** (209 mg, 0.15 mmol), **12** (50 mg, 0.031 mmol) and sodium ascorbate (2 mg, 0.009 mmol) in CH_2Cl_2/H_2O (1/1, 2 mL) at room temperature. The reaction mixture was stirred for 1 h. The organic layer was diluted with CH_2Cl_2, washed with water, dried (Na_2SO_4), filtered and concentrated. Column chromatography (SiO_2, CH_2Cl_2) followed by gel permeation chromatography (Biobeads SX-1 CH_2Cl_2) gave **F–P–F** (98 mg, 64%) as a dark purple glassy product. IR (neat): 1749 (C=O). ^{1}H NMR ($CDCl_3$, 300 MHz): 0.88 (t, $J = 7$ Hz, 24H), 1.20–1.45 (m, 144H), 1.71 (m, 16H), 1.81 (s, 12H), 2.60 (m, 10H), 3.82 (t, $J = 7$ Hz, 16H), 4.12 (m, 4H), 4.80 (m, 4H), 5.11 (d, $J = 13$ Hz, 4H), 5.26 (d, $J = 12$ Hz, 8H), 5.73 (d, $J = 13$ Hz, 4H), 6.33 (m, 4H), 6.44 (d, $J = 2$ Hz, 8H), 6.84 (m, 4H), 7.14 (m, 2H), 7.23 (s, 4H), 8.00 (s, 2H), 8.14 (d, $J = 8$ Hz, 4H), 8.28 (d, $J = 8$ Hz, 4H), 8.75 (d, $J = 5$ Hz, 4H), 8.90 (d, $J = 5$ Hz, 4H). ^{13}C NMR ($CDCl_3$, 75 MHz): 14.0, 21.3, 21.8, 22.8, 26.2, 29.4, 29.5, 29.6, 29.7, 29.8, 29.9, 32.1, 49.37, 64.5, 66.9, 67.2, 68.3, 68.8, 70.7, 101.6, 107.1, 112.1, 115.1, 119.4, 120.0, 123.9, 127.7, 129.9, 130.7, 132.2, 134.6, 135.1, 135.7, 135.9, 137.5, 135.6, 138.7, 139.1, 139.2, 139.8, 140.9, 141.6, 142.7, 142.8, 142.9, 143.1, 143.2, 143.9, 144.0, 144.1, 144.2, 144.6, 144.7, 144.8, 144.9, 145.1, 145.3, 145.4, 145.8, 147.1, 147.2, 147.3, 147.6, 148.5, 149.8, 149.9, 158.9, 160.5, 162.5, 162.6. Anal. Calcd for $C_{332}H_{286}N_{10}O_{26}Zn \cdot 2H_2O$: C 80.83, H 5.92, N 2.84; found: C 80.99, H 6.22, N 2.79%. MALDI-MS: 4898.5 ([M + H]$^+$, calcd for $C_{332}H_{287}N_{10}O_{26}Zn$: 4898.36).

Electrochemistry

The cyclic voltammetric measurements were carried out with a potentiostat Autolab PGSTAT100. Experiments were performed at room temperature in a homemade airtight three-electrode cell connected to a vacuum/argon line. The reference electrode consisted of a saturated calomel electrode (SCE) separated from the solution by a bridge compartment. The counter electrode was a platinum wire of *ca.* 1 cm^2 apparent surface. The working electrode was a Pt microdisk (0.5 mm diameter). The supporting electrolyte [*n*-Bu_4N][BF_4] (Fluka, 99% electrochemical grade) was used as received and simply degassed under argon. Dichloromethane was freshly distilled over CaH_2 prior to use. The solutions used during the electrochemical studies were typically 10^{-3} M in compound and 0.1 M in supporting electrolyte. Before each measurement, the solutions were degassed by bubbling Ar and the working electrode was polished with a polishing machine (Presi P230). Under these experimental conditions, Fc^+/Fc is observed at +0.55 ± 0.01 V *vs.* SCE.

Photophysics

The photophysical studies were carried out in benzonitrile and toluene (Carlo Erba, spectrofluorimetric grade). Absorption spectra were recorded with a Perkin-Elmer Lambda 950 UV/Vis/NIR spectrophotometer. Molar absorption values (ε) were calculated by applying the Lambert–Beer law to the absorbance spectra ($A_{max} < 0.7$) of the compounds.

Steady-state photoluminescence spectra were measured in right angle mode with an Edinburgh FLS920 spectrometer (continuous 450 W Xe lamp), equipped with a Peltier-cooled Hamamatsu R928 photomultiplier tube (185–850 nm) or a Hamamatsu R5509-72 supercooled photomultiplier tube (193 K, 800–1700 nm range). The concentration of air-equilibrated sample solutions was adjusted to obtain absorption values $A <$ 0.15 at the excitation wavelength. Emission quantum yields were determined according to the approach described by Demas and Crosby,[39] using [Ru(bipy)$_3$Cl$_2$] ($\Phi_{em} = 0.028$ in air-equilibrated water solution)[40] as standard. One centimetre path length square optical Suprasil Quartz (QS) cuvettes were used for measurements at RT of dilute solutions, while capillary tubes immersed in liquid nitrogen in a coldfinger quartz Dewar were used for measurements of solvent frozen glasses at 77 K.

Fluorescence lifetimes were measured with an IBH 5000F time-correlated single-photon counting device, by using pulsed NanoLED excitation sources at 331, 373, 465 and 560 nm. Analysis of the luminescence decay profiles against time was accomplished with the Decay Analysis Software DAS6 provided by the manufacturer.

Phosphorescence spectra and decays were measured at 77 K in solvent frozen dilute solutions on a Perkin-Elmer LS-50B spectrofluorimeter equipped with a pulsed Xe lamp and in gated detection mode. The phosphorescence decay analysis was performed with the PHOSDecay software provided by the manufacturer. All spectra are acquired under the same experimental condition.

Transient absorption spectra in the nanosecond–microsecond time domain were obtained by using the nanosecond flash photolysis apparatus Proteus by Ultrafast Systems LLC. The excitation source was a tunable laser system made by a optical parametric oscillator (Continuum Surelite OPO PLUS) pumped by the second harmonic (532 or 355 nm) of a Continuum Surelite II Nd:YAG laser with 5 ns pulse duration at 0.1–10 mJ per pulse. Light signals were passed through a Chromex/Bruker 500IS monochromator (equipped with two gratings blazed at 600 or 1200 nm), and collected on a high-speed Silicon (DET210) or InGaAs (DET410) Thorlabs detector in the Vis (400–800 nm) and NIR (800–1700 nm) regions, respectively. The signal was then amplified by means of a variable gain wideband voltage amplifier (Femto DHPVA-200) interfaced with a Tektronix TDS 3032B digital oscilloscope connected to a PC having the acquisition software Proteus. The probe light source was a 150 W CW Xe Arc lamp Spectra Physics 69907. Triplet lifetimes were obtained by averaging 64 or 132 different decays recorded around the maximum of the absorption peak (*e.g.* 720 nm). The samples were placed in fluorimetric 1 cm path cuvettes and, when necessary, purged from oxygen by at least 4 freeze–thaw–pump cycles. Typical laser power has been taken as 0.5 mJ per pulse which, taking into account the photon energy at 650 nm, the concentration of the sample, and the volume of solution effectively excited, leads to an excitation of about 10% of the overall fullerene molecules, thus making negligible the chance of multiple excitation events within compounds.

All measurements were carried out in spectroscopy grade solvents, used without further purification. Experimental uncertainties are estimated to be 8% for lifetime determinations, 20% for emission quantum yields, 5% for relative emission intensities in the NIR, and <1 and <5 nm for absorption and emission peaks respectively.

Acknowledgements

This research was supported by the CNRS, the University of Strasbourg, the CNR, and the EC (contract PITN-GA-2008-215399—FINELUMEN). J.I. thanks the French Ministry of Research for his fellowship. We further thank A. Saquet for the CV measurements.

Notes and references

1 (*a*) N. Martín, L. Sanchez, B. Illescas and I. Perez, *Chem. Rev.*, 1998, **98**, 2527; (*b*) J.-F. Nierengarten, *New J. Chem.*, 2004, **28**, 1177; (*c*) N. Martín, *Chem. Commun.*, 2006, 2093; (*d*) J. N. Clifford, G. Accorsi, F. Cardinali, J.-F. Nierengarten and N. Armaroli, *C. R. Chim.*, 2006, **9**, 1005; (*e*) T. M. Figueira-Duarte, A. Gégout and J.-F. Nierengarten, *Chem. Commun.*, 2007, 109; (*f*) G. Accorsi and N. Armaroli, *J. Phys. Chem. C*, 2010, **114**, 1385.

2 (*a*) D. Gust, T. A. Moore and A. L. Moore, *Acc. Chem. Res.*, 2001, **34**, 40; (*b*) D. M. Guldi, *Chem. Soc. Rev.*, 2002, **31**, 22; (*c*) D. I. Schuster, K. Li and D. M. Guldi, *C. R. Chim.*, 2006, **9**, 892; (*d*) A. Mateo-Alonso, C. Sooambar and M. Prato, *C. R. Chim.*, 2006, **9**, 944; (*e*) J.-F. Nierengarten, *J. Porphyrins Phthalocyanines*, 2008, **12**, 1022; (*f*) R. Chitta and F. D'Souza, *J. Mater. Chem.*, 2008, **18**, 1440.

3 (*a*) H. Imahori, *J. Phys. Chem. B*, 2004, **108**, 6130; (*b*) H. Imahori, *Org. Biomol. Chem.*, 2004, **2**, 1425; (*c*) H. Imahori and S. Fukuzumi, *Adv. Funct. Mater.*, 2004, **14**, 525; (*d*) S. Fukuzumi and T. Kojima, *J. Mater. Chem.*, 2008, **18**, 1427.

4 H. Imahori, K. Hagiwara, T. Akiyama, M. Aoki, S. Taniguchi, T. Okada, M. Shirakawa and Y. Sakata, *Chem. Phys. Lett.*, 1996, **263**, 545.

5 (*a*) D. I. Schuster, P. D. Jarowski, A. N. Kirschner and S. R. Wilson, *J. Mater. Chem.*, 2002, **12**, 2041–2047; (*b*) N. Solladié, M. E. Walther, M. Gross, T. M. Figueira Duarte, C. Bourgogne and J.-F. Nierengarten, *Chem. Commun.*, 2003, 2412.

6 P. D. W. Boyd and C. A. Reed, *Acc. Chem. Res.*, 2005, **38**, 235 and references therein.

7 (*a*) N. Armaroli, G. Marconi, L. Echegoyen, J.-P. Bourgeois and F. Diederich, *Chem.–Eur. J.*, 2000, **6**, 1629; (*b*) V. Vehmanen, N. V. Tkachenko, H. Imahori, S. Fukuzumi and H. Lemmetyinen, *Spectrochim. Acta, Part A*, 2001, **57**, 2229; (*c*) D. M. Guldi, A. Hirsch, M. Scheloske, E. Dietel, A. Troisi, F. Zerbetto and M. Prato, *Chem.–Eur. J.*, 2003, **9**, 4968; (*d*) A. Hosseini, S. Taylor, G. Accorsi, N. Armaroli, C. A. Reed and P. D. W. Boyd, *J. Am. Chem. Soc.*, 2006, **129**, 15903.

8 (*a*) J.-F. Nierengarten, C. Schall and J.-F. Nicoud, *Angew. Chem., Int. Ed.*, 1998, **37**, 1934; (*b*) J.-F. Nierengarten, L. Oswald and J.-F. Nicoud, *Chem. Commun.*, 1998, 1545; (*c*) M. Urbani and J.-F. Nierengarten, *Tetrahedron Lett.*, 2007, **48**, 8111; (*d*) M. Urbani, J. Iehl, I. Osinska, R. Louis, M. Holler and J.-F. Nierengarten, *Eur. J. Org. Chem.*, 2009, 3715.

9 J. Iehl, I. Osinska, R. Louis, M. Holler and J.-F. Nierengarten, *Tetrahedron Lett.*, 2009, **50**, 2245.

10 For other examples of fullerene–porphyrin conjugates prepared under the copper mediated Huisgen 1,3-dipolar cycloaddition conditions, see: (*a*) J. Iehl, R. Pereira de Freitas, B. Delavaux-Nicot and J.-F. Nierengarten, *Chem. Commun.*, 2008, 2450; (*b*) M. A. Fazio, O. P. Lee and D. I. Schuster, *Org. Lett.*, 2008, **10**, 4979; (*c*) J. D. Megiatto, Jr, R. Spencer and D. I. Schuster, *Org. Lett.*, 2009, **11**, 4152.

11 (*a*) R. Huisgen, *Angew. Chem., Int. Ed. Engl.*, 1968, **7**, 321; (*b*) H. C. Kolb, M. G. Finn and K. B. Sharpless, *Angew. Chem., Int. Ed.*, 2001, **40**, 2004.

12 (*a*) J. Iehl, R. Pereira de Freitas and J.-F. Nierengarten, *Tetrahedron Lett.*, 2008, **49**, 4063; (*b*) R. Pereira de Freitas, J. Iehl, B. Delavaux-Nicot and J.-F. Nierengarten, *Tetrahedron*, 2008, **64**, 11409.

13 For other examples of copper mediated Huisgen 1,3-dipolar cycloaddition reactions from fullerene building blocks, see: (*a*) H. Isobe, K. Cho, N. Solin, D. B. Werz, P. H. Seeberger and E. Nakamura, *Org. Lett.*, 2007, **9**, 4611; (*b*) W.-B. Zhang, Y. Tu, R. Ranjan, R. M. Van Horn, S. Leng, J. Wang, M. J. Polce, C. Wesdemiotis, R. P. Quirk, G. R. Newkome and S. Z. D. Cheng, *Macromolecules*, 2008, **41**, 515; (*c*) I. M. Mahmud, N. Zhou, L. Wang and Y. Zhao, *Tetrahedron*, 2008, **64**, 11420; (*d*) P. Pierrat, S. Vanderheiden, T. Muller and S. Bräse, *Chem. Commun.*, 2009, 1748; (*e*) J. Iehl and J.-F. Nierengarten, *Chem.–Eur. J.*, 2009, **15**, 7306; (*f*) J.-F. Nierengarten, J. Iehl, V. Oerthel, M. Holler, B. M. Illescas, A. Muñoz, N. Martín, J. Rojo, M. Sánchez-Navarro, S. Cecioni, S. Vidal, K. Buffet, M. Durka and S. P. Vincent, *Chem. Commun.*, 2010, **46**, 3860; (*g*) J. Iehl and J.-F. Nierengarten, *Chem. Commun.*, 2010, **46**, 4160; (*h*) P. Compain, C. Decroocq, J. Iehl, M. Holler, D. Hazelard, T. Mena Barragán, C. Ortiz Mellet and J.-F. Nierengarten, *Angew. Chem., Int. Ed.*, 2010, **49**, 5753.

14 (*a*) J.-F. Nierengarten, V. Gramlich, F. Cardullo and F. Diederich, *Angew. Chem., Int. Ed. Engl.*, 1996, **35**, 2101; (*b*) J.-F. Nierengarten, T. Habicher, R. Kessinger, F. Cardullo, F. Diederich, V. Gramlich, J.-P. Gisselbrecht, C. Boudon and M. Gross, *Helv. Chim. Acta*, 1997, **80**, 2238.

15 C. Bingel, *Chem. Ber.*, 1993, **126**, 1957.

16 D. Felder, M. Gutiérrez Nava, M. del Pilar Carreon, J.-F. Eckert, M. Luccisano, C. Schall, P. Masson, J.-L. Gallani, B. Heinrich, D. Guillon and J.-F. Nierengarten, *Helv. Chim. Acta*, 2002, **85**, 288.

17 V. Aucagne, K. V. Hänni, D. A. Leigh, P. J. Lusby and D. B. Walker, *J. Am. Chem. Soc.*, 2006, **128**, 2186.

18 J.-F. Nierengarten and J.-F. Nicoud, *Tetrahedron Lett.*, 1997, **38**, 7737.

19 U. Hahn, F. Cardinali and J.-F. Nierengarten, *New J. Chem.*, 2007, **31**, 1128; M. Holler and J.-F. Nierengarten, *Aust. J. Chem.*, 2009, **62**, 605.

20 S. Zhang, Y. Rio, F. Cardinali, C. Bourgogne, J.-L. Gallani and J.-F. Nierengarten, *J. Org. Chem.*, 2003, **68**, 9787.

21 (*a*) Y. Rio, G. Enderlin, C. Bourgogne, J.-F. Nierengarten, J.-P. Gisselbrecht, M. Gross, G. Accorsi and N. Armaroli, *Inorg. Chem.*, 2003, **42**, 8783; (*b*) F. Cardinali, H. Mamlouk, Y. Rio, N. Armaroli and J.-F. Nierengarten, *Chem. Commun.*, 2004, 1582.

22 (*a*) A. Hirsch, I. Lamparth and H. R. Karfunkel, *Angew. Chem., Int. Ed. Engl.*, 1994, **33**, 437; (*b*) F. Cardullo, P. Seiler, L. Isaacs, J.-F. Nierengarten, R. F. Haldimann, F. Diederich, T. Mordasini-Denti, W. Thiel, C. Boudon, J.-P. Gisselbrecht and M. Gross, *Helv. Chim. Acta*, 1997, **80**, 343.

23 J.-F. Nierengarten, S. Zhang, A. Gégout, M. Urbani, N. Armaroli, G. Marconi and Y. Rio, *J. Org. Chem.*, 2005, **70**, 7550.

24 (*a*) B. J. Littler, Y. Ciringh and J. S. Lindsey, *J. Org. Chem.*, 1999, **64**, 2864; (*b*) G. R. Geier, III, B. J. Littler and J. S. Lindsey, *J. Chem. Soc., Perkin Trans. 2*, 2001, 701.

25 (*a*) R. W. Wagner, D. S. Lawrence and J. S. Lindsey, *Tetrahedron Lett.*, 1987, **28**, 3069; (*b*) J. S. Lindsey and R. W. Wagner, *J. Org. Chem.*, 1989, **54**, 828.

26 (*a*) M. Gutierrez-Nava, G. Accorsi, P. Masson, N. Armaroli and J.-F. Nierengarten, *Chem.–Eur. J.*, 2004, **10**, 5076; (*b*) J.-F. Nierengarten, U. Hahn, A. Trabolsi, H. Herschbach, F. Cardinali, M. Elhabiri, E. Leize, A. Van Dorsselaer and A.-M. Albrecht-Gary, *Chem.–Eur. J.*, 2006, **12**, 3365.

27 M. Holler, F. Cardinali, H. Mamlouk, J.-F. Nierengarten, J.-P. Gisselbrecht, M. Gross, Y. Rio, F. Barigelletti and N. Armaroli, *Tetrahedron*, 2006, **62**, 2060; U. Hahn, E. Maisonhaute, C. Amatore and J.-F. Nierengarten, *Angew. Chem., Int. Ed.*, 2007, **46**, 951.

28 F. Cardullo, P. Seiler, L. Isaacs, J.-F. Nierengarten, R. F. Haldimann, F. Diederich, T. Mordasini-Denti, W. Thiel, C. Boudon, J.-P. Gisselbrecht and M. Gross, *Helv. Chim. Acta*, 1997, **80**, 343; B. Knight, N. Martín, T. Ohno, E. Ortí, C. Rovira, J. Veciana, J. Vidal-Gancedo, P. Viruela, R. Viruela and F. Wudl, *J. Am. Chem. Soc.*, 1997, **119**, 9871; R. Kessinger, J. Crassous, A. Herrmann, M. Rüttimann, L. Echegoyen and F. Diederich, *Angew. Chem., Int. Ed.*, 1998, **37**, 1919; M. W. J. Beulen, L. Echegoyen, J. A. Rivera, M. A. Herranz, A. Martin-Domenech and N. Martin, *Chem. Commun.*, 2000, 917; D. Felder, H. Nierengarten, J.-P. Gisselbrecht, C. Boudon, E. Leize, J.-F. Nicoud, M. Gross, A. Van Dorsselaer and J.-F. Nierengarten, *New J. Chem.*, 2000, **24**, 687.

29 N. Armaroli, G. Accorsi, Y. Rio, P. Ceroni, V. Vicinelli, R. Welter, T. Gu, M. Saddik, M. Holler and J.-F. Nierengarten, *New J. Chem.*, 2004, **28**, 1627.

30 K. M. Kadish, E. van Caemelbecke and G. Royal, in *The Porphyrin Handbook*, ed. K. M. Kadish, K. M. Smith and R. Guilard, Academic Press, San Diego, 1999, vol. 8, pp. 1–114.

31 (*a*) J.-P. Bourgeois, F. Diederich, L. Echegoyen and J.-F. Nierengarten, *Helv. Chim. Acta*, 1998, **81**, 1835; (*b*) T. M. Figueira-Duarte, V. Lloveras, J. Vidal-Gancedo, B. Delavaux-Nicot, C. Duhayon, J. Veciana, C. Rovira and J.-F. Nierengarten, *Eur. J. Org. Chem.*, 2009, 5779.

32 N. Armaroli, F. Diederich, L. Echegoyen, T. Habicher, L. Flamigni, G. Marconi and J.-F. Nierengarten, *New J. Chem.*, 1999, **23**, 77.

33 U. Hahn, J.-F. Nierengarten, F. Voegtle, A. Listorti, F. Monti and N. Armaroli, *New J. Chem.*, 2009, **33**, 337.

34 J. C. Scaiano, R. W. Redmond, B. Mehta and J. T. Arnason, *Photochem. Photobiol.*, 1990, **52**, 655.

35 N. Armaroli, G. Accorsi, F. Song, A. Palkar, L. Echegoyen, D. Bonifazi and F. Diederich, *ChemPhysChem*, 2005, **6**, 732.

36 (*a*) T. W. Ebbesen, K. Tanigaki and S. Kuroshima, *Chem. Phys. Lett.*, 1991, **181**, 501; (*b*) D. K. Palit, A. V. Sapre, J. P. Mittal and C. N. R. Rao, *Chem. Phys. Lett.*, 1992, **195**, 1; (*c*) N. M. Dimitrijevic and P. V. Kamat, *J. Phys. Chem.*, 1992, **96**, 4811.

37 (*a*) A. Osuka, S. Nakajima, T. Okada, S. Taniguchi, K. Nozaki, T. Ohno, I. Yamazaki, Y. Nishimura and N. Mataga, *Angew. Chem., Int. Ed. Engl.*, 1996, **35**, 92; (*b*) J.-H. Fuhrhop and D. Mauzerall, *J. Am. Chem. Soc.*, 1969, **91**, 4174; (*c*) A. N. Acpherson, P. A. Liddell, S. Lin, L. Noss, G. R. Seely, J. M. DeGraziano, A. L. Moore, T. A. Moore and D. Gust, *J. Am. Chem. Soc.*, 1995, **117**, 7202; (*d*) H. Chosrowjan, S. Tanigichi, T. Okada, S. Takagi, T. Arai and K. Tokumaru, *Chem. Phys. Lett.*, 1995, **242**, 644.

38 (*a*) M. A. Greaney and S. M. Gorun, *J. Phys. Chem.*, 1991, **95**, 7142; (*b*) D. Dubois, K. M. Kadish, S. Flanagan, R. E. Haufler, L. P. F. Chibante and L. J. Wilson, *J. Am. Chem. Soc.*, 1991, **113**, 4364.

39 J. N. Demas and G. A. Crosby, *J. Phys. Chem.*, 1971, **75**, 991.

40 S. R. Meech and D. Phillips, *J. Photochem.*, 1983, **23**, 193.